RESEARCH

UCHL1 loss alters the cell cycle in metastatic pancreatic neuroendocrine tumors

Brendan M Finnerty[1],*, Maureen D Moore[1],*, Akanksha Verma[2], Anna Aronova[1], Shixia Huang[3], Dean P Edwards[3], Zhengming Chen[4], Marco Seandel[1], Theresa Scognamiglio[5], Yi-Chieh Nancy Du[5], Olivier Elemento[2], Rasa Zarnegar[1], Irene M Min[1] and **Thomas J Fahey III[1]**

[1]Department of Surgery, Weill Cornell Medicine, New York, New York, USA
[2]Department of Physiology and Biophysics, Weill Cornell Medicine, New York, New York, USA
[3]Dan L. Duncan Cancer Center and Department of Molecular and Cellular Biology, Baylor College of Medicine, One Baylor Plaza, Houston, Texas, USA
[4]Department of Healthcare Policy & Research, Weill Cornell Medicine, New York, New York, USA
[5]Department of Pathology & Laboratory Medicine, Weill Cornell Medicine, New York, New York, USA

Correspondence should be addressed to B M Finnerty: bmf9002@med.cornell.edu

*(B M Finnerty and M D Moore contributed equally to this work)

Abstract

Loss of ubiquitin carboxyl-terminal hydrolase L1 (UCHL1) expression by CpG promoter hypermethylation is associated with metastasis in gastroenteropancreatic neuroendocrine tumors; however, the mechanism of how UCHL1 loss contributes to metastatic potential remains unclear. In this study, we first confirmed that the loss of UCHL1 expression on immunohistochemistry was significantly associated with metastatic tumors in a translational pancreatic neuroendocrine tumor (PNET) cohort, with a sensitivity and specificity of 78% and 89%, respectively. To study the mechanism driving this aggressive phenotype, BON and QGP-1 metastatic PNET cell lines, which do not produce UCHL1, were stably transfected to re-express UCHL1. *In vitro* assays, RNA sequencing and reverse phase protein array (RPPA) analyses were performed comparing empty-vector negative controls and UCHL1-expressing cell lines. UCHL1 re-expression is associated with lower anchorage-independent colony growth in BON cells, lower colony formation in QGP cells and a higher percentage of cells in the G0/G1 cell-cycle phase in BON and QGP cells. On RPPA proteomic analysis, there was an upregulation of cell-cycle regulatory proteins CHK2 (1.2-fold change, $P = 0.004$) and P21 (1.2-fold change, $P = 0.023$) in BON cells expressing UCHL1; western blot confirmed upregulation of phosphorylated CHK2 and P21. There were no transcriptomic differences detected on RNA sequencing between empty-vector negative controls and UCHL1-expressing cell lines. In conclusion, UCHL1 loss correlates with metastatic potential in PNETs and its re-expression induces a less aggressive phenotype *in vitro*, in part by inducing cell-cycle arrest through posttranslational regulation of phosphorylated CHK2. UCHL1 expression should be considered as a functional biomarker in detecting PNETs capable of metastasis.

Introduction

Pancreatic neuroendocrine tumors (PNETs) are rare tumors comprising only 2% of all pancreatic tumors, with a twofold increase in incidence since 1975 (Halfdanarson *et al.* 2008, Lawrence *et al.* 2011). The role of genetic alterations associated with familial inherited syndromes and the development of PNETs have been well defined, such as in the multiple endocrine neoplasia (MEN) and von Hippel–Lindau (VHL) syndromes. However, the genetic profile of sporadic PNETs, which are more common, is less clear as their tumorigenesis does not appear to be controlled by classic oncogenes such as *P53*, *RB* or *KRAS* (Yoshimoto *et al.* 1992, Yashiro *et al.* 1993, Chung *et al.* 1997). More recent studies have elucidated *MEN1* and *DAXX/ATRX* mutations in sporadic PNETs, as well as alterations in the mTOR pathway (Jiao *et al.* 2011) and angiogenic growth factors (Fjällskog *et al.* 2003). This has led to the clinical success of the targeted mTOR inhibitor everolimus (Yao *et al.* 2011) and multi-kinase inhibitor sunitinib (Raymond *et al.* 2011) for metastatic PNETs. However, progression-free survival is limited to 11 months in these phase 3 trials, thus there are other factors contributing to malignant transformation and tumor progression.

Diagnostically, Ki-67 proliferation index is the best available biomarker associated with aggressive behavior in PNETs and is a key component to current tumor grading (Klimstra *et al.* 2010, Díaz Del Arco *et al.* 2017). However, PNETs have a wide variability of metastatic potential, and well-differentiated tumors can present with an advanced stage independent of Ki-67 index (Alexiev *et al.* 2009, Miller *et al.* 2014). In an effort to identify more accurate biomarkers of metastatic potential in PNETs, our group has previously shown that the loss of ubiquitin carboxyl-terminal hydrolase L1 (UCHL1) expression by CpG promoter hypermethylation is associated with metastasis in gastroenteropancreatic neuroendocrine tumors (GEP-NETs) (Kleiman *et al.* 2014). UCHL1 is a posttranslational modifier that de-ubiquitinates proteins otherwise destined for lysosomal degradation (Brinkmann *et al.* 2013). The role of UCHL1 in tumorigenesis is controversial as there is conflicting evidence regarding its dual tumorigenic or tumor suppressive properties depending upon cancer type. Its overexpression has been implicated in the metastatic potential of gastric adenocarcinoma, potentially by activating the mitogenic and anti-apoptotic ERK/AKT pathway (Gu *et al.* 2015*a*, Yang *et al.* 2015).

On the other hand, UCHL1 has been reported to be silenced by promoter hypermethylation in breast (Xiang *et al.* 2012), nasopharyngeal (Li *et al.* 2010, Loyo *et al.* 2011), esophageal (Mandelker *et al.* 2005), renal cell (Seliger *et al.* 2009), colorectal (Okochi-Takada *et al.* 2006), ovarian (Okochi-Takada *et al.* 2006) and prostate carcinomas (Ummanni *et al.* 2011). It has been described as a tumor suppressor in breast and nasopharyngeal carcinomas by stabilizing p53 levels and inducing cell-cycle arrest (Li *et al.* 2010, Xiang *et al.* 2012). UCHL1 has also been shown in prostate cancer cell lines to suppress growth by P53-mediated inhibition of AKT/PKB phosphorylation, as well as via accumulation of CDKN1B, a cyclin-dependent kinase inhibitor of cell-cycle regulating proteins, through a separate pathway dependent on cyclin A activity (Ummanni *et al.* 2011).

Our aim was to confirm UCHL1 loss specifically in PNETs and to elucidate the mechanism by which UCHL1 silencing may contribute to a more aggressive phenotype by re-expressing UCHL1 in the PNET cell lines, BON and QGP-1. Herein, we report that UCHL1 expression promotes a less aggressive phenotype *in vitro* as evaluated by anchorage-independent growth, cell migration and cell invasion assays. We demonstrate through differential protein expression analysis that these changes are likely, in part, secondary to UCHL1 inducing cell-cycle arrest by increased activation of phosphorylated CHK2, a cell-cycle regulator.

Materials and methods

Patients and tumor tissue

A prospectively maintained clinicopathologic and tissue database was reviewed to identify patients who had undergone surgery for a PNET at a single academic, tertiary care referral center between 2007 and 2015. Unstained 5 μM-thick, formalin-fixed, paraffin-embedded slides of tumor from these patients were obtained for immunohistochemistry (described below). Clinicopathologic factors were compared between localized and metastatic tumors, specifically, age, sex, tumor size, location and timing of metastasis, vascular invasion, perineural invasion, Ki-67 index and UCHL1 immunohistochemical (IHC) staining. The Weill Cornell Medicine Institutional Review Board approved this study and patient consent was obtained for the prospective protocol.

IHC staining and grading

IHC staining of UCHL1 was accomplished using the BOND III Autostainer (Leica Microsystems). Formalin-fixed, paraffin-embedded tissue sections were first baked and deparaffinized. Antigen retrieval was followed by heating the slides at 99–100°C in BOND Epitope Retrieval Solution 1 for 30 min. Sections were subjected to sequential incubations with primary antibody (anti-PGP9.5 rabbit polyclonal, 1:200 dilution, Dako), postprimary antibody (equivalent to secondary antibody), polymer (equivalent to tertiary antibody), endogenous peroxidase block, diaminobenzidine (DAB) and hematoxylin for 15, 8, 8, 5, 10 and 5 min (Bond Polymer Refine Detection; Leica Microsystems), respectively. The sections were dehydrated in 100% ethanol and mounted in Cytoseal XYL (Richard-Allan Scientific, Kalamazoo, MI, USA).

Grading of UCHL1 IHC was performed by a gastrointestinal endocrine pathologist (T S) based on the extent of staining within the tumor. Staining was categorized as either absent, <50% or ≥50% – tumors with ≥50% staining were considered high for UCHL1 expression. These results were correlated with the presence or absence of metastatic disease.

Cell culture

BON cells were originally derived from a localized metastatic lymph node adjacent to a PNET (Parekh *et al.* 1994) and have no natural UCHL1 expression (Supplementary Fig. 1A, see section on supplementary data given at the end of this article). Cell line authenticity was confirmed by short-tandem repeat profiling (American Type Culture Collection) as compared to prior studies (Silva *et al.* 2011, Vandamme *et al.* 2015); stock passage number 21 was used for experimentation. QGP-1 cells were derived from a primary metastatic pancreatic islet cell tumor (Kaku *et al.* 1980) and have no UCHL1 expression (Supplementary Fig. 1A). Cell line authenticity was confirmed by short-tandem repeat profiling (American Type Culture Collection) as compared to the DSMZ Profile Database; stock passage number 12 was used for experimentation. Cells were grown in RPMI-1640 media (Sigma-Aldrich) supplemented with 10% fetal bovine serum (FBS) and 1% penicillin/streptomycin/amphotericin (P/S/A) and incubated at 37°C in a 5% CO_2 environment. Cells were routinely subcultured and medium was changed every 2–3 days. For particular experiments specified below, serum-free RPMI-1640 supplemented with 1% P/S/A or medium with 2.5% FBS was utilized for specific durations.

Transfection of cell lines

BON cells with stable, inducible expression of UCHL1 (BON/UCHL1) via a PiggyBac cumate-switch promoter (System Biosciences, Mountain View, CA, USA) were generated per manufacturer protocol as follows. The cDNA for human *UCHL1*-PiggyBac was co-transfected with a PiggyBac transposase plasmid into BON cells using Lipofectamine (Life Technologies) in Opti-MEM (Life Technologies). After 1 week, cells were subject to selection with puromycin for two weeks and expanded. As a negative control, an empty-vector BON cell line was also generated using the same transposase protocol without a *UCHL1* gene insert (BON/Empty). Cells were treated for 72 h with 60 μg/mL cumate to achieve maximal stable expression of UCHL1 (Supplementary Fig. 1B).

The QGP-1 cell line was stably transfected with the *UCHL1* gene using the Fugene HD Transfection Kit (Promega) and pCDNA3.1 plasmid vector according to the manufacturer's instructions (QGP/UCHL1). Briefly, 3×10^5 cells were plated in a 6-well dish overnight in RPMI medium with 10% FBS. Subsequently, 6 μg of plasmid was added to the Fugene HD/serum-free RPMI combination at a 3:1 (DNA: Fugene) ratio, then mixed and incubated at room temperature for 15 min. The mixture of Fugene HD and plasmid DNA was then added to cells cultured in 3 mL fresh serum-free RPMI and incubated at 37°C in 5% CO_2. After 24 h post transfection, the transfection reagent was replaced with fresh culture medium; 48 h later, the transfected cells were passaged and treated with Geneticin selection medium. A total of six QGP/UCHL1 clones were generated. As controls, eight empty vector clones (QGP/Empty) were also generated. Of note, QGP/UCHL1 clones 4 and 5 demonstrated strong UCHL1 expression and were used for experimentation, as were QGP-empty vector clones 3 and 4. All experimentation was performed in at least triplicates.

Cell proliferation assay

The Vybrant MTT Cell Proliferation Assay Kit (Thermo Scientific) was used to assess cell proliferation and growth curves. For this experiment, 7000 viable cells were seeded in a final volume of 100 μL of phenol-free media per well in four 96-well plates (one plate per time point). Every 24 h, all media were replaced; one plate was subjected to the assay by adding 10 μL of 12 mM MTT stock solution, as per manufacturer's instructions. In brief, the plate was incubated at 37°C for 4 h, after which all but 25 μL was removed and 50 μL of dimethyl sulfoxide (DMSO)

(Sigma-Aldrich) was added to each well. The plate was incubated at 37°C for an additional 10 min and absorbance was read in a microplate reader (iMARK; Bio-Rad) at 490 nM.

Cell-cycle analysis

For cell-cycle analysis, 1×10^6 cells were seeded in 6-well plates overnight. Media were replaced with 2.5% media in a subset of wells the following morning and cells were harvested and fixed after 48 h of low-serum culture by utilizing cold phosphate-buffered solution (PBS) and 70% cold ethanol, respectively. After fixation at 4°C overnight, cells were washed twice with PBS, treated with 100 μg/mL RNaseA for 30 min at 4°C, washed once with PBS, stained with 50 μg/mL propidium iodide (PI) and transferred to fresh polystyrene tubes through a 70-micron nylon filter to remove cell clumps. The cells were analyzed by flow cytometry (Gallios; Beckman Coulter, Brea, CA, USA) and cell-cycle stages were determined using the Kaluza software (Beckman Coulter). Each experiment was performed with at least 20,000 events per sample for analysis.

Apoptosis analysis

For apoptosis analyses, the PE Annexin V Apoptosis Detection Kit was used (BD Biosciences, San Jose, CA, USA) according to the manufacturer's instructions. A total of 1×10^6 cells were seeded in 6-well plates overnight. Cells were washed with PBS and 1×10^5 cells were re-suspended in 1X Binding Buffer. The cells were then stained with Annexin V-PE and 7-AAD, vortexed, incubated at room temperature for 15 min in the dark and analyzed by flow cytometry as above.

Cell migration assay

A scratch assay was used to assess for cell migration *in vitro*. A total of 4×10^5 cells were seeded in 6-well plates and grown to ~60–80% confluence. A 200 μL pipette tip was used to create a horizontal scratch across the plate at three locations. Complete media was changed every 3 days. Cells were photographed daily and percent migration was measured at six marked fields using ImageJ software.

Cell invasion assay

The extent of cell invasion was assessed with the Corning BioCoat Matrigel Invasion Chambers 24-well Cell Invasion Assay (Corning Inc.) according to the manufacturer's

instructions. A total of 2×10^5 cells in serum-free media were seeded onto inserts (8 μM pore-sized pre-coated extracellular basement membrane). The inserts were placed in a 24-well plate containing 10% FBS media. The plates were incubated for 24 h at 37°C. Cells that invaded the matrix to the lower surface of the membrane were fixed and stained with 0.1% crystal violet solution and counted. Invaded cells from four high-powered fields in four separate quadrants of each membrane were counted under a light microscope and averaged.

Soft agar anchorage-independent growth assay

Two-layered soft agar assays were performed in 6-well plates. The bottom layer of agar (1 mL/well) contained 0.5% agar (Sigma-Aldrich) in maintenance medium. A total of 25,000 cells in maintenance medium were mixed with warm agarose at 37°C for a 0.35% solution and allowed to solidify atop the agar layer. This was then overlaid with 2 mL complete media and allowed to grow at 37°C in 5% CO_2. Media was changed twice every week. After 3 weeks of culture, cell colonies were stained with 0.005% crystal violet solution and examined by microscopy. Individual colonies were counted in four separate fields per well and summed for each of the six replicates.

Colony formation assay

Experimental and empty-vector control cells were plated in a 6-well plate (1000 cells/well) and cultured with fresh media for 5–7 days at 37°C in 5% CO_2. Colonies were fixed with methanol and stained with 0.1% crystal violet and examined by microscopy. This was performed in triplicate and repeated three times.

RNA extraction and next-generation RNA sequencing

RNA was extracted from BON and QGP-1 cells using the RNeasy Mini Kit (Qiagen) according to the manufacturer's instructions. RNA quality was assessed with a Bioanalyzer (Agilent Technologies). An RNA integrity number (RIN) of ≥8 was required for library preparation. Samples were prepared for next-generation sequencing with the TruSeq RNA sample prep kit (Illumina, San Diego, CA, USA). Paired-end cluster generation was performed utilizing the TruSeq SBS Kit v3-Hs in conjunction with the TruSeq PE Cluster Kit v3-cBot-HS on the HiSeq2000 (Illumina). Illumina HiSeq control software performed a real-time analysis of the sequencing runs. Three samples were run in each lane using paired-end mode

(2×51 cycles). Reads were aligned to the UCSC human genome (Version GRCH37/hg19) using TopHat v2.0.12 (Trapnell *et al.* 2012) (http://ccb.jhu.edu/software/tophat/index.shtml) with default parameters. Aligned reads were then quantified against the reference annotation (hg19 from UCSC) to obtain FPKM (Fragments per Kilobase per million) and raw counts using Cufflinks v2.2.1 (http://cole-trapnell-lab.github.io/cufflinks/) and HTseq (https://htseq.readthedocs.io/en/release_0.11.1/), respectively (Trapnell *et al.* 2010, Anders *et al.* 2015). Differential gene expression was performed on voom transformed raw counts using the Limma package in R (Law *et al.* 2014). Genes with a false discovery rate (FDR) of ≤0.10 are being considered significant.

Protein preparation and western blot analysis

Protein was extracted with Radioimmunoprecipitation Assay (RIPA) Lysis buffer (Santa Cruz Biotechnology). Protein concentration was determined by the Pierce BCA assay method according to the manufacturer's protocol (Thermo Scientific). Western blots were performed with 10 µg protein per lane using semi-dry transfer and horseradish-peroxidase (HRP)-conjugated antigen retrieval system as described previously (Kleiman *et al.* 2013). The nitrocellulose membranes were probed with the following primary antibodies: UCHL1 (D3T2E) (#13179), CHK2 (1C12) (#3440), phosphorylated-CHK2 (Thr68) (2661) (Cell Signaling Technology), β-tubulin (ab6046), β-actin (ab8229) and anti-GAPDH (EPR16891) (ab181602) (Abcam).

Reverse phase protein array analysis

Reverse phase protein array (RPPA) analysis was used to generate a differential protein expression profile between BON cells producing UCHL1 compared to its empty vector; the assays were carried out as previously described (Creighton & Huang 2015, Holdman *et al.* 2015). Protein lysates were prepared from BON/Empty and BON/UCHL1 cells in quadruplicate, using tissue protein extraction reagent (Thermo Scientific) supplemented with 450 mM NaCl and a cocktail of protease and phosphatase inhibitors (Sigma-Aldrich). Protein lysates were denatured in sodium dodecyl sulfate (Invitrogen) containing 2-mercaptoethanol (Sigma-Aldrich) at 100°C for 8 min. The Aushon 2470 Arrayer (Aushon BioSystems, Billerica, MA, USA) was used to spot lysates onto nitrocellulose-coated slides (Grace Biolabs, Bend, OR, USA) using an array format of 960 lysates/slide with each sample spotted

as technical triplicates including test and control lysates. Antibody labeling was performed at room temperature with an automated slide stainer Autolink 48 (Dako); each slide was incubated with primary and secondary antibodies, as well as Vectastain-ABC Streptavidin-Biotin Complex (Vector, PK-6100) and TSA-plus Biotin Amp Reagent (PerkinElmer) for signal amplification. A fluorescent detection signal was generated by incubating slides with LI-COR IRDye 680 Streptavidin (Odyssey, Lincoln, NE, USA) and assessed using Sypro Ruby Protein Blot Stain (Molecular Probes). Slides were scanned on a GenePix AL4200 microarray scanner and images were analyzed with GenePix Pro 7.0 (Molecular Devices, Sunnyvale, CA, USA). Total fluorescence signal intensities were obtained and normalized for variation in total protein, background and non-specific labeling using a group-based normalization method as described previously (Grubb *et al.* 2009). The replicates of each normalized sample were log$_2$-transformed and then averaged before analysis. The Linear Regression Model from Limma R package (https://bioconductor.org/packages/release/bioc/html/limma.html) was used to identify the differentially expressed proteins between treatment and control (BON/UCHL vs BON/Empty, respectively) (Ritchie *et al.* 2015). Benjamini–Hochberg procedure was used to adjust the *P* values to control the FDR; an adjusted *P* value < 0.1 was considered significant.

There are a total of 204 validated antibodies for RPPA, which represent proteins in signaling pathways and cell functionality such as growth factor receptors, cell cycle, cell proliferation, apoptosis, EMT, stem cells, DNA damage, cell stress, autophagy, cytokines, protein translation and gene transcriptional regulators. Of these, 132 antibodies detect total protein and 72 detect specific phosphorylated states of proteins known to be markers of protein activation states. Antibody validation for RPPA was performed using an immunoblot assay of multiple known positive and negative controls as described previously (Holdman *et al.* 2015).

Statistical analysis

Calculations to determine significance in all experiments except RNA sequencing and RPPA protein analyses (for which the methods are described above) were carried out using Pearson's chi-squared test, Student's *t*-test, Mann–Whitney U-test, one-way analysis of variance or Kruskal–Wallis test, as appropriate. Continuous variables that followed a normal distribution are presented as mean ± standard deviation (s.d.), while those that were not

normally distributed are presented as median (interquartile range (IQR)). A *P* value of <0.05 was considered statistically significant. All statistical analyses (except those performed for transcriptomics and proteomics, as described above) were performed using STATA version 13.0 (StataCorp, College Station, TX, USA).

Results

Loss of IHC staining for UCHL1 is associated with metastatic tumors

In order to confirm in a PNET cohort the prior finding that metastatic GEP-NETs are associated with loss of UCHL1 (Kleiman *et al.* 2014), we performed IHC staining for UCHL1 on 16 well-differentiated primary PNETs (nine localized, seven metastatic) with Ki-67 <20%. Additionally, we included two liver neuroendocrine metastases of pancreatic origin for staining. On univariable analysis of the primary PNETs, there were no differences in age or sex between localized and metastatic groups; however, the metastatic cohort was significantly associated with larger mean tumor size, vascular invasion, perineural invasion, higher Ki67 index and loss of UCHL1 staining (Table 1). The sample size was too small to perform a multivariable analysis. Additionally, loss of UCHL1 had a sensitivity, specificity, negative predictive value and positive predictive value of 78, 89, 88, and 80%, respectively, of detecting metastatic disease in the entire cohort. UCHL1 IHC staining <50%, including absence of staining, was significantly associated with increased risk of metastasis (*P*<0.016) (Fig. 1 and Table 1).

Table 1 Patient demographics and tumor characteristics of primary PNETs (localized vs metastatic).

	M0 (*n* = 9)	**M1** (*n* = 7)	***P* value**
Age (years)	63 ± 20	64 ± 16	0.15
Male	7 (78%)	3 (43%)	0.09
Tumor size (cm)	2.1 ± 1.1	3.4 ± 2.4	0.03
Location of metastasis			
Locoregional	–	4 (57%)	–
Distant		3 (43%)	
Timing of metastasis			
Initial presentation	–	6 (86%)	–
Late		1 (14%)	
Vascular invasion	0 (0%)	3 (43%)	0.02
Perineural invasion	0 (0%)	3 (43%)	0.02
UCHL1 staining (<50%)	1 (11%)	5 (71%)	0.01
Ki67 index	2.5 ± 1.9	8.6 ± 6.5	0.03

M0, patients without metastatic disease; M1, patients with metastatic disease.
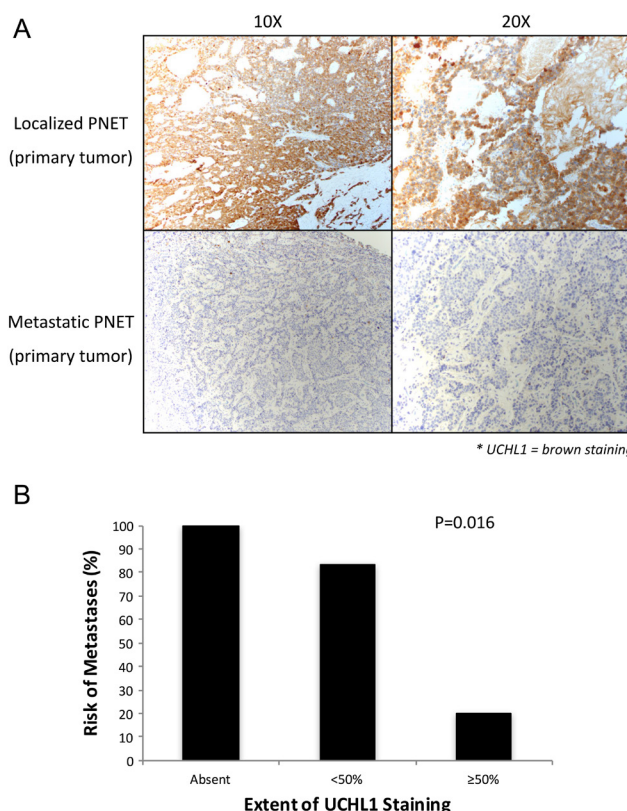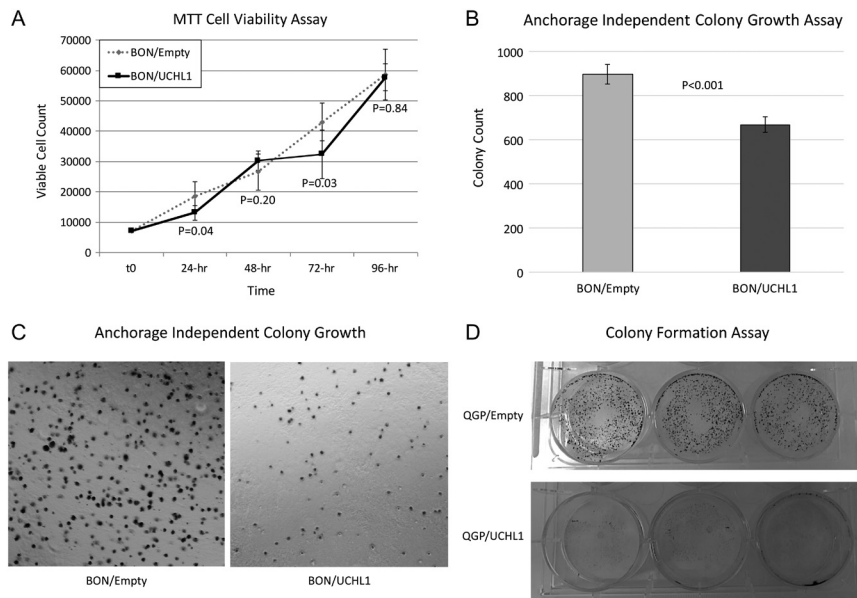
Figure 1
Loss of UCHL1 expression by immunohistochemical staining is associated with metastatic pancreatic neuroendocrine tumors, as compared to localized tumors (A). Extent of UCHL1 <50% is associated with a significant risk of metastasis (B). A full color version of this figure is available at https://doi.org/10.1530/ERC-18-0507.

UCHL1 re-expression induces less aggressive phenotype in BON and QGP-1 cells

Since silencing of UCHL1 is associated with metastatic PNETs, we aimed to investigate the phenotypic effects that occur upon UCHL1 re-expression in the PNET cell lines BON and QGP-1, which do not produce UCHL1 (Supplementary Fig. 1). We specifically evaluated cellular proliferation/viability, anchorage-independent colony growth, migration and invasion. Of note, BON/UCHL1 cells treated with cumate in media achieved a maximal stable expression of UCHL1 after 48 to 72 h (Supplementary Fig. 2), thus the 't0' for all BON cell line experimentation below was at 72 h of cumate treatment.

There were no differences in cellular viability comparing BON/UCHL1 to BON/Empty cells, as assessed by MTT assay at 96 h of growth (Fig. 2A). However, BON/UCHL1 cells demonstrated less anchorage-independent colony growth after 3 weeks as compared to BON/Empty (Fig. 2B and C). Specifically, and notably,

Figure 2
BON cell viability was not affected upon UCHL1 re-expression (A). Anchorage-independent colony growth in BON cells was significantly lower upon UCHL1 re-expression (B and C). Colony growth formation was less in QGP-1 cells re-expressing UCHL1 (D).

there was a lower mean anchorage-independent colony count in the BON/UCHL1 group compared to BON/Empty (668±36 vs 895±43, *P*<0.001). Additionally, QGP/UCHL1 showed markedly less growth compared to QGP/Empty in a colony formation assay (Fig. 2D).

Furthermore, BON/UCHL1 demonstrated decreased migration as assessed in scratch (Fig. 3A and B) and cellular invasion (Fig. 3C) assays. Specifically, in the BON/UCHL1 group, there was a lower mean percent leading-edge migration in the scratch assay after 96h of growth (11.8±1.8% vs 23.1±2.0%, *P*<0.001) and a

lower mean number of invaded cells in the Matrigel assay (35±6 vs 61±12, *P*=0.028).

In summary, UCHL1 re-expression reduces anchorage-independent growth, as well as cellular invasion and migration of PNET cell lines, most notably in the BON cell line.

UCHL1 re-expression affects cell cycle but not apoptosis

In order to examine the mechanism causing the above noted cellular growth changes, we evaluated cell cycle
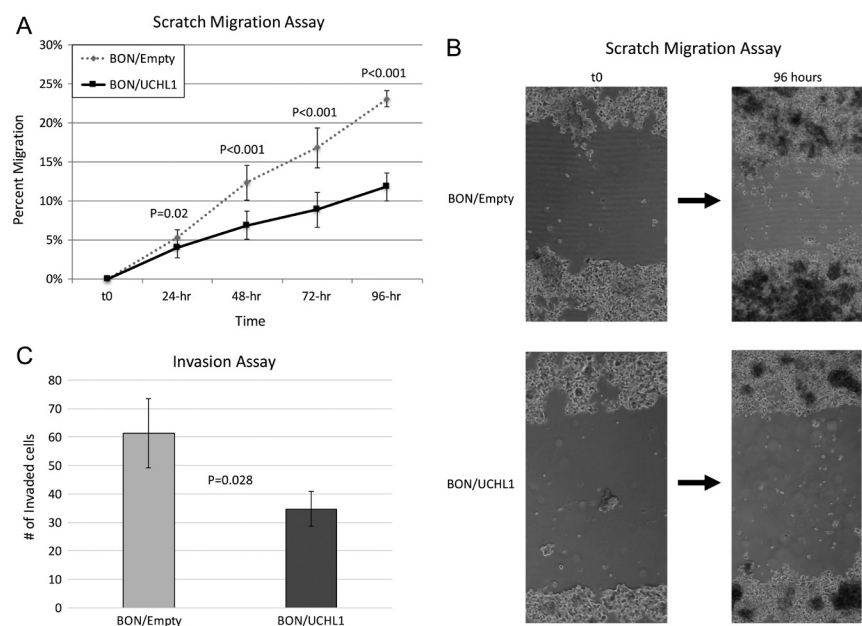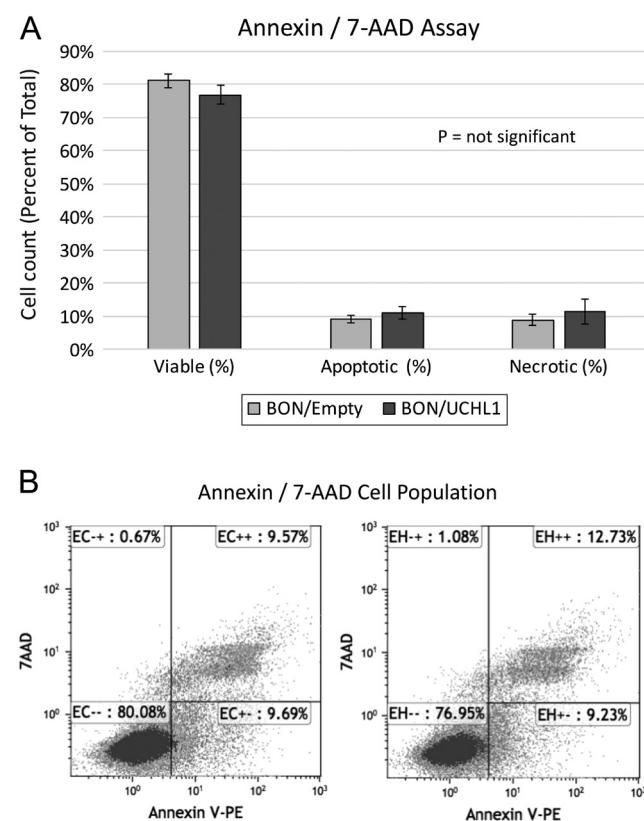

Figure 3
Slower BON cell migration was observed upon UCHL1 re-expression (A and B). BON cells demonstrated less invasion in the Matrigel assay (C).

and apoptotic differences between BON/UCHL1 and BON/Empty cells. Using an Annexin V and 7-AAD assay, there were no differences in apoptotic, necrotic or viable cells between groups (Fig. 4A and B). However, using a PI cell-sorting assay, we detected a change in cell-cycle phases between BON/UCHL1 and BON/Empty (Fig. 5A). Specifically, there was an increase in percentage of cells arrested in the G0/G1 phase in BON/UCHL1 compared to BON/Empty (45±6% vs 36±5%, *P*=0.039). This is associated with a decline in cells in S and G2/M in the BON/UCHL1 group as seen in the cell-cycle plot (Fig. 5B). These findings were also observed in the QGP-1 cell line, where there was a higher percentage of QGP/UCHL1 cells in G0/G1 compared to QGP/Empty (70±5% vs 61±4%, *P*=0.009) (Fig. 5A and C).

UCHL1 re-expression does not have major transcriptomic effects in BON cells

We utilized next-generation RNA sequencing to investigate if the observed changes in growth, migration and invasion

Figure 4
Apoptotic, necrotic and viable cell populations were not affected by UCHL1 re-expression in BON cells (A), as depicted in a representative Annexin/7-AAD flow cytometry plot (B).
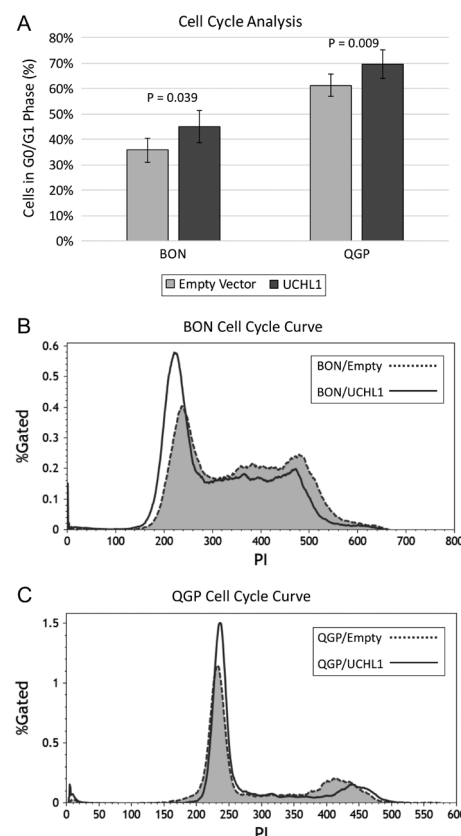
Figure 5
BON and QGP cells demonstrated a shift to the G0/G1 phase upon UCHL1 re-expression (A), as depicted in representative BON (B) and QGP (C) flow cytometry plots. Of note, QGP was grown in stressed low-serum media with 2.5% fetal bovine serum.

associated with UCHL1 re-expression are accompanied by alterations at the gene expression level. Differential gene expression profiling was performed on extracted RNA from BON/UCHL1 and BON/Empty. Only five genes were differentially expressed between cell lines, none of which have widely known oncogenic implications, particularly with relation to cell cycle, migration or invasion (Table 2). Notably, somatostatin (SST) was downregulated in BON/UCHL1 with a log-fold change of −1.39 (adj *P* value 0.0763). Lastly, *UCHL1* gene expression was expectedly the most differentially expressed gene with a log-fold change of 10 compared between BON/UCHL1 and BON/Empty.

RPPA analysis identifies CHK2 as the most differentially upregulated protein in BON/UCHL1

Since UCHL1 did not appear to exert any transcriptional effects in BON/UCHL1 as compared to BON/Empty and has also been demonstrated to be a posttranslational

Table 2 Differential gene expression between BON/UCHL1 and BON/Empty.

Gene	Log-fold change	P value	Adjusted P value
UCHL1	9.62	2.45 E-07	0.0016
MS4A8	−1.06	1.01 E-05	0.0452
SST	−1.39	2.85 E-05	0.0763
MEP1A	−1.28	7.78 E-05	0.0872
DDC	−1.07	8.24 E-05	0.0872
C2orf54	−1.02	5.37 E-05	0.0872

modifier, we next aimed to evaluate protein expression and phosphorylation changes with UCHL1 expression in the BON cells. To develop a differential protein expression/phosphorylation profile of molecules integral in cell signaling and growth, BON/Empty and BON/UCHL1 cell lysates were prepared for RPPA analysis. As described in 'Materials and methods', this protocol allows for the evaluation of 204 proteins using validated antibodies including those implicated in cell cycle, cell proliferation, apoptosis, DNA damage, cell stress, protein translation and gene transcriptional regulators, and others.

When comparing BON/UCHL1 to BON/Empty, there were 23 differentially expressed proteins (Table 3). CHK2, a cell-cycle regulator, was the most differentially

Table 3 Differential protein expression between BON/UCHL1 and BON/Empty.

Protein	Fold change[a]	P value	Adjusted P value
CHK2	1.21	2.0E-05	0.0042
FOS	1.41	6.3E-05	0.0044
MAP1LC3B	1.32	4.3E-05	0.0044
HK2	0.75	0.00010	0.0052
RPS6KB1	1.39	0.00026	0.0107
LAMC2	0.72	0.00032	0.0110
MAP1LC3A	1.21	0.00085	0.0232
CDKN1A (P21)	1.20	0.00089	0.0232
JUN	1.36	0.00200	0.0327
CDKN1B (P27)	1.28	0.00159	0.0327
MAP2K6	1.17	0.00220	0.0327
MYC	0.90	0.00211	0.0327
FOXO1	0.87	0.00168	0.0327
STAT6	0.87	0.00184	0.0327
PRKAA1, PRKAA2	1.20	0.00237	0.0329
MAP2K1	0.84	0.00276	0.0359
ITGA4	0.69	0.00339	0.0415
EPAS1	0.82	0.00361	0.0418
TP53	1.19	0.00677	0.0712
MKI67	1.14	0.00685	0.0712
MTOR	1.12	0.00795	0.0788
RRM2	1.17	0.01059	0.0981
AURKA, AURKB, AURKC	1.13	0.01085	0.0981

[a]Fold change >1 is upregulation whereas fold change <1 is downregulation in BON/UCHL1.

upregulated protein in BON/UCHL1 (adjusted P value = 0.0042). There were a total of four upregulated cell-cycle proteins with adjusted P value <0.1, including P21, phosphorylated P27 and phosphorylated P53. Other notable downregulated potentially oncogenic proteins in BON/UCHL1 included FOS, JUN, MYC, FOXO1 and STAT6. Interestingly, two proteins in the mTOR pathway were upregulated (RPS6KB1, MTOR). Lastly, integrin alpha-4 (ITGA4), a protein implicated in cellular migration, was downregulated in BON/UCHL1.

Phosphorylated CHK2 is confirmed to be upregulated in cells expressing UCHL1

In order to confirm the findings from the RPPA analysis, we performed western blots for total CHK2, phosphorylated CHK2 (p-CHK2) and P21 in BON/UCHL1, QGP/UCHL1 and their respective negative control cell lines with empty vector (Fig. 6). We found that total CHK2 did not differ between BON/UCHL1 and BON/Empty as well as between QGP/UCHL1 and QGP/Empty. However, more notably, the activated p-CHK2 was increased in both BON/UCHL1 and QGP/UCHL1 compared to their empty vector controls. Furthermore, the p-CHK2 downstream target P21 was upregulated in BON/UCHL1. This was not observed in QGP/UCHL1, possibly secondary to the relatively low log-fold change in our RPPA analysis, as well as the observation that QGP-1 is a more slowly growing cell line.

Discussion

The ubiquitin-proteasome pathway is an important regulator of intracellular protein stability. It is a crucial pathway for posttranslational modifications critical to normal cellular processes, and its disturbances contribute to tumorigenesis (Mani & Gelmann 2005). UCHL1 is a widely studied deubiquitinase as it has been described in both neurodegenerative disorders and varying malignancies (Sacco *et al.* 2010). Depending on tumor types, some studies report *UCHL1* as an oncogene, whereas others discuss its role as a tumor suppressor gene as a result of CpG island methylation (Okochi-Takada *et al.* 2006, Leiblich *et al.* 2007, Yu *et al.* 2008, Kim *et al.* 2009, Kleiman *et al.* 2014, Abdelmaksoud-Dammak *et al.* 2016). Our group previously reported in a translational cohort of GEP-NETs that UCHL1 was silenced via hypermethylation of promoter CpG islands and was further identified as an independent predictor of metastatic disease
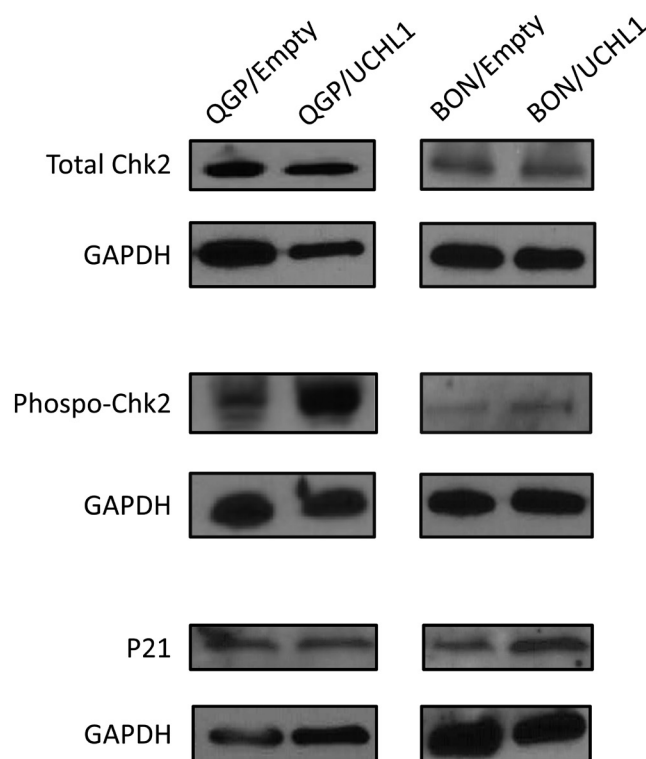
Figure 6
Western blots separately confirming cell-cycle proteins' expression in BON and QGP upon UCHL1 re-expression, including total CHK2, phosphorylated-CHK2 and P21.

(Kleiman *et al.* 2014). The mechanisms behind how UCHL1 loss contributes to the malignant potential of PNETs has remained elusive.

In this study, we sought to determine the functional consequences of re-expression of UCHL1 in PNET cell lines, as disruptions in the ubiquitin-proteasome pathway can lead to decreased tumor suppressor proteins, enhanced oncogenic properties, epithelial-mesenchymal transitions and alterations in cell-cycle progression and migration (Fraile *et al.* 2012). Upon UCHL1 re-expression, we observed a decrease in anchorage-independent cell growth, colony formation, cellular migration and cellular invasion. Functionally, re-expression of UCHL1 *in vitro* induced a shift toward G0/G1 cell-cycle arrest, without involvement of the apoptotic cascade. To investigate the mechanism that would explain these functional changes, we analyzed the transcriptomic and proteomic changes induced by UCHL1 re-expression. Our RNA-sequencing data do not suggest a change in the transcriptome of cell-cycle regulatory genes upon re-expression of UCHL1. However, the proteomic changes detected by our RPPA analysis suggest that the G0/G1 cell-cycle shift may be regulated by the posttranslational effects of UCHL1.

Thus, the functional consequence of cell-cycle arrest in BON and QGP-1 cell lines re-expressing UCHL1 may explain the phenotypic changes noted, most importantly in the anchorage-independent growth assay and the colony formation assay.

The two most differentially expressed cell-cycle proteins in our RPPA analysis were upregulation of CHK2 and P21 in UCHL1-expressing cells. We further confirmed that p-CHK2 is increased in BON and QGP-1, and P21 is increased in BON, after re-expression of UCHL1. CHK2 is multifunctional kinase that is critical in cell-cycle regulation (Bartek *et al.* 2001). Mutations of *CHK2* and variations of CHK2 protein expression have not been previously reported in PNETs; however, mutations in *CHK2* have been described in breast cancer (Wang *et al.* 2015). During DNA damage response, phosphorylation of CHK2 occurs, converting the protein into its active state and thus initiating the transduction of DNA damage checkpoint signals (Cai *et al.* 2009). Specifically, CHK2 functions upstream of other cell-cycle regulators such as P53 and P21, especially during DNA damage (Hirao *et al.* 2000). By triggering cell-cycle arrest upon irreparable DNA damage, CHK2 may help to suppress tumor progression (Bartkova *et al.* 2005). With regard to UCHL1 and cell cycle, a report by Xiang *et al.* studied its role in breast tumorigenesis and found that UCHL1 displays tumor suppressive functions by inducing G0/G1 arrest through P53 accumulation (Xiang *et al.* 2012). Similarly, in nasopharyngeal carcinoma cell lines, UCHL1 expression has been shown to increase protein expression of P53 and P21 while decreasing expression of MDM2, thus promoting cell-cycle arrest and apoptosis (Li *et al.* 2010).

In addition to the G0/G1 cell-cycle phase shift, the induction of UCHL1 expression also led to decreased cellular migration and decreased cellular invasiveness, suggesting an additional mechanism of tumor suppressor function. We have yet to characterize the downstream factors associated with the decreased cell migration and invasion in PNETs; however, our RPPA analysis shows that cells re-expressing UCHL1 have an associated decrease of integrin alpha-4, a protein involved in cellular migration. Contrary to our migration and invasion results, Kim *et al.* reported that high UCHL1 expression in non-small cell lung cancer cell line H157 resulted in increased invasive potential with corresponding changes in cell morphology through cell adhesion molecule pathways such as AKT (Kim *et al.* 2009). Similar findings have been observed in gastric adenocarcinoma cell lines – increased UCHL1 expression has been associated with increased migration and invasion, likely by altering the AKT and ERK1/2 pathways

(Gu *et al.* 2015*b*). Interestingly, the AKT pathway has been shown as an important modulator of tumor growth in BON and QGP-1, particularly in the setting of mTOR and PI3K-mTOR inhibition (Zitzmann *et al.* 2010, Vandamme *et al.* 2016). Our data suggests there may be some effect of UCHL1 expression and the mTOR pathway; however, it remains unclear how this is related to the changes in cell cycle we observed in this study. Overall, current reports continue to suggest that UCHL1 exerts a wide variety of tumorigenic or tumor suppressive effects based on tumor cell type, which implies that UCHL1 likely has different deubiquitinase targets dependent on cell type.

Lastly, our data show that loss of UCHL1 expression on IHC staining is significantly associated with metastatic tumors in a PNET cohort, with a sensitivity and specificity of 78% and 89%, respectively. This suggests that loss of UCHL1 expression should be further investigated as a translational marker for aggressive disease in order to aid in clinical decision-making.

Our study has several limitations. Most notably, while our RPPA analysis did yield significant results, the absolute fold change was low. This may explain why we were able to confirm upregulation of P21 by western blot only in the BON cell line. The QGP-1 cell line is slow growing and difficult to maintain; thus, our phenotypic experimentation was largely reliant on the BON cell line. However, we were able to confirm the G0/G1 cell-cycle shift in both cell lines, as well as the p-CHK2 protein expression changes, which corroborate our main observations. Given these limitations, our next steps include verifying the phenotypic changes we observed *in vitro* in a mouse model, and specifically observing rates of metastases in tumors expressing UCHL1 compared to those that do not.

In summary, this study demonstrates that re-expression of UCHL1 exerts tumor suppressive functions in PNET cell lines by decreasing colony formation and overall metastatic potential through cell-cycle changes modulated by p-CHK2. Our study further contributes to the growing body of literature that the tumor suppressor effects of UCHL1 are likely through posttranslational control of oncogenic pathways, and not necessarily at a transcriptional level. Further studies are warranted to identify downstream targets of UCHL1 that may explain the increased cell migration and cell invasion. Lastly, as loss of UCHL1 expression identified on immunohistochemistry is associated with metastatic disease, its utility as both a clinical biomarker and potential therapeutic target in metastatic PNETs should be further investigated in prospective cohorts.

References

Abdelmaksoud-Dammak R, Saadallah-Kallel A, Miladi-Abdennadher I, Ayedi L, Khabir A, Sallemi-Boudawara T, Frikha M, Daoud J & Mokdad-Gargouri R 2016 CpG methylation of ubiquitin carboxyl-terminal hydrolase 1 (UCHL1) and P53 mutation pattern in sporadic colorectal cancer. *Tumour Biology* **37** 1707–1714. (https://doi.org/10.1007/s13277-015-3902-4)

Alexiev BA, Darwin PE, Goloubeva O & Ioffe OB 2009 Proliferative rate in endoscopic ultrasound fine-needle aspiration of pancreatic endocrine tumors: correlation with clinical behavior. *Cancer* **117** 40–45. (https://doi.org/10.1002/cncy.20014)

Anders S, Pyl PT & Huber W 2015 HTSeq—a Python framework to work with high-throughput sequencing data. *Bioinformatics* **31** 166–169. (https://doi.org/10.1093/bioinformatics/btu638)

Bartek J, Falck J & Lukas J 2001 CHK2 kinase – a busy messenger. *Nature Reviews Molecular Cell Biology* **2** 877–886. (https://doi.org/10.1038/35103059)

Bartkova J, Horejsí Z, Koed K, Krämer A, Tort F, Zieger K, Guldberg P, Sehested M, Nesland JM, Lukas C, *et al*. 2005 DNA damage response as a candidate anti-cancer barrier in early human tumorigenesis. *Nature* **434** 864–870. (https://doi.org/10.1038/nature03482)

Brinkmann K, Zigrino P, Witt A, Schell M, Ackermann L, Broxtermann P, Schüll S, Andree M, Coutelle O, Yazdanpanah B, *et al*. 2013 Ubiquitin C-terminal hydrolase-L1 potentiates cancer chemosensitivity by stabilizing NOXA. *Cell Reports* **3** 881–891. (https://doi.org/10.1016/j.celrep.2013.02.014)

Cai Z, Chehab NH & Pavletich NP 2009 Structure and activation mechanism of the CHK2 DNA damage checkpoint kinase. *Molecular Cell* **35** 818–829. (https://doi.org/10.1016/j.molcel.2009.09.007)

Chung DC, Smith AP, Louis DN, Graeme-Cook F, Warshaw AL & Arnold A 1997 Analysis of the retinoblastoma tumour suppressor gene in pancreatic endocrine tumours. *Clinical Endocrinology* **47** 523–528. (https://doi.org/10.1046/j.1365-2265.1997.2861110.x)

Creighton CJ & Huang S 2015 Reverse phase protein arrays in signaling pathways: a data integration perspective. *Drug Design, Development and Therapy* **9** 3519–3527. (https://doi.org/10.2147/DDDT.S38375)

Díaz Del Arco C, Esteban López-Jamar JM, Ortega Medina L, Díaz Pérez JÁ & Fernández Aceñero MJ 2017 Fine-needle aspiration biopsy of pancreatic neuroendocrine tumors: correlation between Ki-67 index in cytological samples and clinical behavior. *Diagnostic Cytopathology* **45** 29–35. (https://doi.org/10.1002/dc.23635)

Fjällskog MLH, Lejonklou MH, Öberg KE, Eriksson BK & Janson ET 2003 Expression of molecular targets for tyrosine kinase receptor antagonists in malignant endocrine pancreatic tumors. *Clinical Cancer Research* **9** 1469–1473.

Fraile JM, Quesada V, Rodríguez D, Freije JM & López-Otín C 2012 Deubiquitinases in cancer: new functions and therapeutic options. *Oncogene* **31** 2373–2388. (https://doi.org/10.1038/onc.2011.443)

Grubb RL, Deng J, Pinto PA, Mohler JL, Chinnaiyan A, Rubin M, Linehan WM, Liotta LA, Petricoin EF & Wulfkuhle JD 2009 Pathway biomarker profiling of localized and metastatic human prostate cancer reveal metastatic and prognostic signatures. *Journal of Proteome Research* **8** 3044–3054. (https://doi.org/10.1021/pr8009337)

Gu YY, Yang M, Zhao M, Luo Q, Yang L, Peng H, Wang J, Huang SK, Zheng ZX, Yuan XH, *et al*. 2015*a* The de-ubiquitinase UCHL1 promotes gastric cancer metastasis via the Akt and ERK1/2 pathways. *Tumour Biology* **36** 8379–8387. (https://doi.org/10.1007/s13277-015-3566-0)

Gu YY, Yang M, Zhao M, Luo Q, Yang L, Peng H, Wang J, Huang SK, Zheng ZX, Yuan XH, *et al*. 2015*b* The de-ubiquitinase UCHL1 promotes gastric cancer metastasis via the Akt and ERK1/2 pathways. *Tumour Biology* **36** 8379–8387. (https://doi.org/10.1007/s13277-015-3566-0)

Halfdanarson TR, Rabe KG, Rubin J & Petersen GM 2008 Pancreatic neuroendocrine tumors (PNETs): incidence, prognosis and recent trend toward improved survival. *Annals of Oncology* **19** 1727–1733. (https://doi.org/10.1093/annonc/mdn351)

Hirao A, Kong YY, Matsuoka S, Wakeham A, Ruland J, Yoshida H, Liu D, Elledge SJ & Mak TW 2000 DNA damage-induced activation of p53 by the checkpoint kinase Chk2. *Science* **287** 1824–1827. (https://doi.org/10.1126/science.287.5459.1824)

Holdman XB, Welte T, Rajapakshe K, Pond A, Coarfa C, Mo Q, Huang S, Hilsenbeck SG, Edwards DP, Zhang X, *et al*. 2015 Upregulation of EGFR signaling is correlated with tumor stroma remodeling and tumor recurrence in FGFR1-driven breast cancer. *Breast Cancer Research* **17** 141. (https://doi.org/10.1186/s13058-015-0649-1)

Jiao Y, Shi C, Edil BH, de Wilde RF, Klimstra DS, Maitra A, Schulick RD, Tang LH, Wolfgang CL, Choti MA, *et al*. 2011 DAXX/ATRX, MEN1, and mTOR pathway genes are frequently altered in pancreatic neuroendocrine tumors. *Science* **331** 1199–1203. (https://doi.org/10.1126/science.1200609)

Kaku M, Nishiyama T, Yagawa K & Abe M 1980 Establishment of a carcinoembryonic antigen-producing cell line from human pancreatic carcinoma. *Gan* **71** 596–601.

Kim HJ, Kim YM, Lim S, Nam YK, Jeong J, Kim HJ & Lee KJ 2009 Ubiquitin C-terminal hydrolase-L1 is a key regulator of tumor cell invasion and metastasis. *Oncogene* **28** 117–127. (https://doi.org/10.1038/onc.2008.364)

Kleiman DA, Buitrago D, Crowley MJ, Beninato T, Veach AJ, Zanzonico PB, Jin M, Fahey TJ & Zarnegar R 2013 Thyroid stimulating hormone increases iodine uptake by thyroid cancer cells during BRAF silencing. *Journal of Surgical Research* **182** 85–93. (https://doi.org/10.1016/j.jss.2012.08.053)

Kleiman DA, Beninato T, Sultan S, Crowley MJP, Finnerty B, Kumar R, Panarelli NC, Liu YF, Lieberman MD, Seandel M, *et al*. 2014

Silencing of UCHL1 by CpG promoter hyper-methylation is associated with metastatic gastroenteropancreatic well-differentiated neuroendocrine (carcinoid) tumors. *Annals of Surgical Oncology* **21** S672–S679. (https://doi.org/10.1245/s10434-014-3787-2)

Klimstra DS, Modlin IR, Coppola D, Lloyd RV & Suster S 2010 The pathologic classification of neuroendocrine tumors: a review of nomenclature, grading, and staging systems. *Pancreas* **39** 707–712. (https://doi.org/10.1097/MPA.0b013e3181ec124e)

Law CW, Chen Y, Shi W & Smyth GK 2014 voom: precision weights unlock linear model analysis tools for RNA-seq read counts. *Genome Biology* **15** R29. (https://doi.org/10.1186/gb-2014-15-2-r29)

Lawrence B, Gustafsson BI, Chan A, Svejda B, Kidd M & Modlin IM 2011 The epidemiology of gastroenteropancreatic neuroendocrine tumors. *Endocrinology and Metabolism Clinics of North America* **40** 1–18, vii. (https://doi.org/10.1016/j.ecl.2010.12.005)

Leiblich A, Cross SS, Catto JW, Pesce G, Hamdy FC & Rehman I 2007 Human prostate cancer cells express neuroendocrine cell markers PGP 9.5 and chromogranin A. *Prostate* **67** 1761–1769. (https://doi.org/10.1002/pros.20654)

Li L, Tao Q, Jin H, Van Hasselt A, Poon FF, Wang X, Zeng MS, Jia WH, Zeng YX, Chan ATC, *et al*. 2010 The tumor suppressor UCHL1 forms a complex with p53/MDM2/ARF to promote p53 signaling and is frequently silenced in nasopharyngeal carcinoma. *Clinical Cancer Research* **16** 2949–2958. (https://doi.org/10.1158/1078-0432.CCR-09-3178)

Loyo M, Brait M, Kim MS, Ostrow KL, Jie CC, Chuang AY, Califano JA, Liegeois NJ, Begum S, Westra WH, *et al*. 2011 A survey of methylated candidate tumor suppressor genes in nasopharyngeal carcinoma. *International Journal of Cancer* **128** 1393–1403. (https://doi.org/10.1002/ijc.25443)

Mandelker DL, Yamashita K, Tokumaru Y, Mimori K, Howard DL, Tanaka Y, Carvalho AL, Jiang WW, Park HL, Kim MS, *et al*. 2005 PGP9.5 promoter methylation is an independent prognostic factor for esophageal squamous cell carcinoma. *Cancer Research* **65** 4963–4968. (https://doi.org/10.1158/0008-5472.CAN-04-3923)

Mani A & Gelmann EP 2005 The ubiquitin-proteasome pathway and its role in cancer. *Journal of Clinical Oncology* **23** 4776–4789. (https://doi.org/10.1200/JCO.2005.05.081)

Miller HC, Drymousis P, Flora R, Goldin R, Spalding D & Frilling A 2014 Role of Ki-67 proliferation index in the assessment of patients with neuroendocrine neoplasias regarding the stage of disease. *World Journal of Surgery* **38** 1353–1361. (https://doi.org/10.1007/s00268-014-2451-0)

Okochi-Takada E, Nakazawa K, Wakabayashi M, Mori A, Ichimura S, Yasugi T & Ushijima T 2006 Silencing of the UCHL1 gene in human colorectal and ovarian cancers. *International Journal of Cancer* **119** 1338–1344. (https://doi.org/10.1002/ijc.22025)

Parekh D, Ishizuka J, Townsend CM, Haber B, Beauchamp RD, Karp G, Kim SW, Rajaraman S, Greeley GJ & Thompson JC 1994 Characterization of a human pancreatic carcinoid in vitro: morphology, amine and peptide storage, and secretion. *Pancreas* **9** 83–90 (https://doi.org/10.1097/00006676-199401000-00013).

Raymond E, Dahan L, Raoul JL, Bang YJ, Borbath I, Lombard-Bohas C, Valle J, Metrakos P, Smith D, Vinik A, *et al*. 2011 Sunitinib malate for the treatment of pancreatic neuroendocrine tumors. *New England Journal of Medicine* **364** 501–513. (https://doi.org/10.1056/NEJMoa1003825)

Ritchie ME, Phipson B, Wu D, Hu Y, Law CW, Shi W & Smyth GK 2015 limma powers differential expression analyses for RNA-sequencing and microarray studies. *Nucleic Acids Research* **43** e47–e47. (https://doi.org/10.1093/nar/gkv007)

Sacco JJ, Coulson JM, Clague MJ & Urbé S 2010 Emerging roles of deubiquitinases in cancer-associated pathways. *IUBMB Life* **62** 140–157. (https://doi.org/10.1002/iub.300)

Seliger B, Handke D, Schabel E, Bukur J, Lichtenfels R & Dammann R 2009 Epigenetic control of the ubiquitin carboxyl terminal hydrolase

1 in renal cell carcinoma. *Journal of Translational Medicine* **7** 90. (https://doi.org/10.1186/1479-5876-7-90)

Silva SR, Bowen KA, Rychahou PG, Jackson LN, Weiss HL, Lee EY, Townsend CM & Evers BM 2011 VEGFR-2 expression in carcinoid cancer cells and its role in tumor growth and metastasis. *International Journal of Cancer* **128** 1045–1056. (https://doi.org/10.1002/ijc.25441)

Trapnell C, Williams BA, Pertea G, Mortazavi A, Kwan G, van Baren MJ, Salzberg SL, Wold BJ & Pachter L 2010 Transcript assembly and quantification by RNA-Seq reveals unannotated transcripts and isoform switching during cell differentiation. *Nature Biotechnology* **28** 511–515. (https://doi.org/10.1038/nbt.1621)

Trapnell C, Roberts A, Goff L, Pertea G, Kim D, Kelley DR, Pimentel H, Salzberg SL, Rinn JL & Pachter L 2012 Differential gene and transcript expression analysis of RNA-seq experiments with TopHat and Cufflinks. *Nature Protocols* **7** 562–578. (https://doi.org/10.1038/nprot.2012.016)

Ummanni R, Jost E, Braig M, Lohmann F, Mundt F, Barett C, Schlomm T, Sauter G, Senff T, Bokemeyer C, *et al.* 2011 Ubiquitin carboxyl-terminal hydrolase 1 (UCHL1) is a potential tumour suppressor in prostate cancer and is frequently silenced by promoter methylation. *Molecular Cancer* **10** 129. (https://doi.org/10.1186/1476-4598-10-129)

Vandamme T, Peeters M, Dogan F, Pauwels P, Van Assche E, Beyens M, Mortier G, Vandeweyer G, de Herder W, Van Camp G, *et al.* 2015 Whole-exome characterization of pancreatic neuroendocrine tumor cell lines BON-1 and QGP-1. *Journal of Molecular Endocrinology* **54** 137–147. (https://doi.org/10.1530/JME-14-0304)

Vandamme T, Beyens M, De Beeck KO, Dogan F, Van Koetsveld PM, Pauwels P, Mortier G, Vangestel C, de Herder W, Van Camp G, *et al.* 2016 Long-term acquired everolimus resistance in pancreatic neuroendocrine tumours can be overcome with novel PI3K-AKT-mTOR inhibitors. *British Journal of Cancer* **114** 650–658. (https://doi.org/10.1038/bjc.2016.25)

Wang N, Ding H, Liu C, Li X, Wei L, Yu J, Liu M, Ying M, Gao W, Jiang H, *et al.* 2015 A novel recurrent CHEK2 Y390C mutation identified in high-risk Chinese breast cancer patients impairs its activity and is associated with increased breast cancer risk. *Oncogene* **34** 5198–5205. (https://doi.org/10.1038/onc.2014.443)

Xiang T, Li L, Yin X, Yuan C, Tan C, Su X, Xiong L, Putti TC, Oberst M, Kelly K, *et al.* 2012 The ubiquitin peptidase UCHL1 induces G0/G1 cell cycle arrest and apoptosis through stabilizing p53 and is frequently silenced in breast cancer. *PLOS ONE* **7** e29783. (https://doi.org/10.1371/journal.pone.0029783)

Yang H, Zhang C, Fang S, Ou R, Li W & Xu Y 2015 UCH-LI acts as a novel prognostic biomarker in gastric cardiac adenocarcinoma. *International Journal of Clinical and Experimental Pathology* **8** 13957–13967.

Yao JC, Shah MH, Ito T, Bohas CL, Wolin EM, Van Cutsem E, Hobday TJ, Okusaka T, Capdevila J, de Vries EG, *et al.* 2011 Everolimus for advanced pancreatic neuroendocrine tumors. *New England Journal of Medicine* **364** 514–523. (https://doi.org/10.1056/NEJMoa1009290)

Yashiro T, Fulton N, Hara H, Yasuda K, Montag A, Yashiro N, Straus F, Ito K, Aiyoshi Y & Kaplan EL 1993 Comparison of mutations of ras oncogene in human pancreatic exocrine and endocrine tumors. *Surgery* **114** 758–763; discussion 763.

Yoshimoto K, Iwahana H, Fukuda A, Sano T, Saito S & Itakura M 1992 Role of p53 mutations in endocrine tumorigenesis: mutation detection by polymerase chain reaction-single strand conformation polymorphism. *Cancer Research* **52** 5061–5064.

Yu J, Tao Q, Cheung KF, Jin H, Poon FF, Wang X, Li H, Cheng YY, Röcken C, Ebert MP, *et al.* 2008 Epigenetic identification of ubiquitin carboxyl-terminal hydrolase L1 as a functional tumor suppressor and biomarker for hepatocellular carcinoma and other digestive tumors. *Hepatology* **48** 508–518. (https://doi.org/10.1002/hep.22343)

Zitzmann K, Rüden Jv von, Brand S, Göke B, Lichtl J, Spöttl G & Auernhammer CJ 2010 Compensatory activation of Akt in response to mTOR and Raf inhibitors – a rationale for dual-targeted therapy approaches in neuroendocrine tumor disease. *Cancer Letters* **295** 100–109. (https://doi.org/10.1016/j.canlet.2010.02.018)